# Flow Measurements in a Model Ramjet Secondary Combustion Chamber

Lazar T. Chittilapilly,* S. Venkateswaran,† P. J. Paul,‡ and H. S. Mukunda§
*Indian Institute of Science, Bangalore, India*

**Experimental studies were conducted on a typical secondary combustion chamber of a ramjet to understand the influence of various inlet parameters such as primary nozzle configuration, secondary air injection angle, and flow Reynolds numbers on the secondary combustion chamber (SCC) performance. Cold flow studies were made with air as the flow medium for both primary and secondary jets followed by similar studies with hot primary jets. The general flow structure in the SCC obtained from surface oil film technique showed recirculation zones near the head end. The combustor length required for jet mixing was found to be unrelated to recirculation zone length confirmed by selective temperature and total pressure profile measurements. The calculated frictional loss from the momentum balance consideration was found to be small. That significant improvement in mixing can be achieved by a choice of multiple-hole primary nozzle configuration has been demonstrated.**



## Nomenclature

$A$ = area
$C_{mom}$ = momentum loss coefficient
$C_p$ = static pressure coefficient
$D$ = diameter of the combustion chamber
$F$ = momentum
$L$ = length of the combustion chamber
$\dot{m}$ = mass flow rate
$P$ = pressure
$pcd$ = pitch circle diameter
$Re$ = Reynolds number
$\rho$ = density
$\theta$ = dump angle
$\eta_{mix}$ = mixing efficiency

*Subscripts*

$c$ = combustion chamber
$e$ = exit
$f$ = frictional
in = inlet
$p$ = primary
$s$ = secondary
$w$ = wall

## Introduction

AIR-AUGMENTED rocket engines combine the performance characteristics of both the rocket and ramjet engines. In the integral ramjet engine, the fuel rich gases from the primary combustion chamber and the ram air from the atmosphere (secondary) are mixed and burned in the secondary combustion chamber (SCC) to obtain thrust. An efficient combustion chamber is one where complete mixing and combustion of the fuel (with air) takes place with a minimum combustor length and pressure loss. Experimental studies are important in evaluating the influence of major parameters such as primary nozzle geometry, dump angle, Reynolds number, etc., on the performance of the combustor. The flow in the combustor is complex, and hence an understanding of the flow phenomena is necessary.

Straight axisymmetric sudden expansion dump combustion chambers have received the most study. In this geometry, the fuel is injected into air before it is dumped into the SCC. Buckley and Obleskid[1] report that swirl given to air before dumping enhances mixing and thereby reduces the required length of the SCC by a factor of two.

In the SCC with coaxial, parallel injection of primary and secondary gases, the loss of radial momentum is avoided at the cost of delayed mixing.[3] The length required for 90% combustion in such a system is of the order of 7-8 diameters compared to 5-6 for the case of radial secondary injection into the combustor.[4] Theoretical downstream pressure calculations of Hsia and Dunlap,[5] assuming no wall friction, gave results close to the experimental values. This agreement is also reported by Masuya et al.[6] for coaxial jets.

In the case of a multiple secondary jet SCC, the secondary jets are injected at an angle to the combustor axis. Work has been carried out on two different modes of primary injection, namely the indirect and direct primary modes.[4,7-9] In the indirect primary mode,[4,7] the fuel is injected into the secondary air inlet ports, whereas in the direct primary mode fuel is injected directly into the SCC. Using a two-dimensional geometry, Greenberg and Timnat[7] studied the indirect primary mode with and without reaction and found that the flow pattern and recirculation zone length was independent of reaction.

Ishikawa[8] conducted experimental investigations with and without a bluff body in the combustion chamber on a two-dimensional model in the direct primary mode. The presence of a bluff body was found to delay mixing. The possible reason for this behavior could be that the increased velocity created by the bluff body delays the mixing, and this overshadows the effect of cross velocity created by the body. Tsujikado,[9] from his experiments on primary injection mode SCC, reported that the length needed for combustion is only two diameters. This length seems to be unusually small compared to the results of other investigations as well as our results. Some investigators[5,10] have attempted one-dimensional analysis of the flow inside SCC to obtain conditions at the inlet and exit of the chamber. The chamber was assumed to be long enough for complete mixing and burning. Ramanujachari et al.[10] calculated chamber exit conditions assuming a frictional loss coefficient of 4 in the combustion chamber, the value given for ramjet the combustion chamber with flame holders. This seems to be an overestimate in the light of the

Received Feb. 20, 1987; revision received June 13, 1989. 

*ME Student, Joint Advanced Technology Program; currently, Engineer, VSSC, Trivandrum.
†Scientific Officer, Joint Advanced Technology Program; currently, Engineer, Lockheed Aerospace Co., Hampton, VA.
‡Assistant Professor, Joint Advanced Technology Program.
§Professor, Joint Advanced Technology Program.

findings of Hsia and Dunlap[5] and Masuya et al.[6] and the present study.

## Present Study

The present study has been carried out on a typical SCC having multiple secondary jets (four numbers) and direct primary mode injection. Tests were conducted with both the primary and secondary nozzles supplied with air at ambient temperature. Selected tests were also performed with primary air being heated to 130°C for different secondary air angles, primary nozzle configurations, and Reynolds numbers selectively. [Some confirmatory tests at higher temperatures (500°C) were also made, but detailed measurements were restricted to jet at 130°C.] An attempt to understand the flow structure with multiple primary and secondary jets has led to a primary nozzle configuration giving fast mixing.

### Experimental Apparatus

The schematic diagram of the air supply scheme is shown in Fig. 1. The air supply was provided by a reciprocating compressor which supplies air at 0.2 kg/s and a pressure of 0.5 MPa. The air supply was divided into two parts: one part for the primary air and the other part for the secondary air. The secondary air was taken through a distributor containing choked nozzles to distribute equally among the four secondary inlets. The primary jet is heated by either an electrical heater of 3 kW or a separate liquefied petroleum gases (LPG) burner for getting higher temperature. Detailed temperature profile measurements were made only while using electrical heating since the temperature obtained using burner was oscillatory. Because of facility restrictions, the Reynolds number (based on diameter of combustion chamber) was limited to $2.7 \times 10^5$.

Figure 2 shows the details of the combustion chamber and the primary nozzles used. Since the primary nozzle configurations were not axisymmetric, the effect of azimuthal position of the primary nozzle with respect to the secondary was also studied. One of the two chosen positions is shown as case A in Fig. 2. The other position is the one in which the primary nozzle is rotated to coincide BB with AA and is denoted as case B.

The choice of dump angles was based on the fact that the extremes of 0 and 90 deg would not be of any practical interest in view of extremes in mixing length and pressure loss. Only two dump angles at 25 and 35 deg were attempted.

Twenty wall pressure taps were provided on the combustor along the axial direction, and three taps were located on the combustor dome. The dome taps were located between two secondary jets at equal distances along the contour of the dome wall. The static pressures were read on a manometer bank.

Stagnation temperatures at the inlet and other points were measured using chromel-alumel thermocouple probes of 0.3 mm bead size. The thermocouples and total pressure probes were mounted on a rake, which could be rotated and moved in the axial direction so that radial, azimuthal, and axial profiles of these quantities could be obtained.

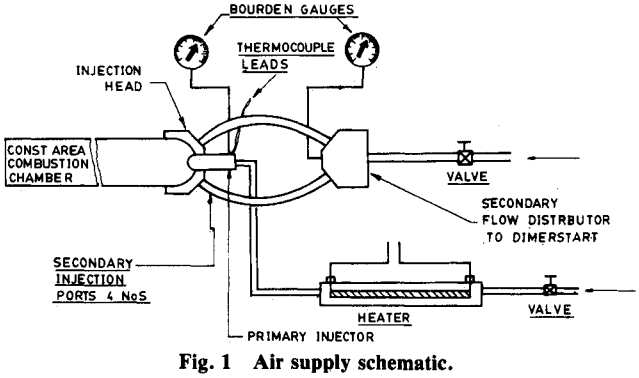


**Fig. 1 Air supply schematic.**

### Flow Visualization

For surface flow visualization, small dots of lamp black suspended in lubricating oil SAE 40 were deposited on the combustor wall prior to the test. This gave flow patterns clearly showing the direction of the flow. Defining the proper mixture having enough fluidity, a long drying time, and which was not affected by gravity required several trials. To facilitate the visualization study, the constant area part of the combustor was made in two halves that could be split open horizontally. The dots were deposited on transparent epoxy sheets at close intervals, and the sheets were glued to the inner side of the combustor wall. The test run time ranged from 30 s to 2 min depending on the flow rates. After each run the epoxy sheets were removed, and the flow pattern was documented by photocopying.

## Results and Discussion

### Surface Flow Pattern

The surface flow patterns for a few typical cases are given in Fig. 3. From the shape of the trail left by the oil-lamp black mixture, which has head and tail identification, the direction of the surface flow can be clearly seen. Regions of reversed flow can be observed near the head end of the combustor. These reverse flow regions can be clearly distinguished in the case of higher Reynolds number flows. However, for low Reynolds numbers, there seems to be a swirl component in the velocity in the recirculation zone, which makes it difficult to locate the point of attachment.

For higher Reynolds number flows, which are of interest, the flow becomes attached within an $L/D$ of 1.5 along each one of the secondary jets. These attachment points can be easily deduced from the flow patterns (see Fig. 3) and look similar to source points from where the flow is issued in all directions along the wall surface. From these results it can be inferred that the flow is approaching these points almost radially.

The surface flow pattern for the single-central-hole primary jet is almost the same (figure not shown) as that for a multiple-hole primary jet showing almost the same recirculation length (1-1.5$D$). This implies that the recirculation length is not indicative of the jet mixing length.

### Wall Static Pressure

The static pressure measurements were made both in line with a secondary jet and between two adjacent secondary jets. In Fig. 4, typical static pressure variations along the combustor are shown for single-hole and the multiple-hole configurations 2 and 4 shown in Fig. 5. Nondimensionalized static pressure variation $C_p$ [defined as $C_p = (P_w - P_e)/(\rho V^2/2)$] is plotted as a function of $x/D$ for a few selected cases. The wall static pressure reaches a maximum at about an $x/D = 4.5$ for the case of the multiple-hole nozzle 2 and then decreases with increasing chamber length. In the case of single-hole primary nozzle, the wall static pressure does not reach a maximum as in the case of multiple-hole nozzle discussed above. This is understood to be due to delayed mixing in the single-hole case compared to the multiple-hole geometry. In the fore of the combustor, the primary jet creates a region of high velocity and consequently a region of low static pressure. The static pressure keeps rising along the combustor length because of the reduction in the core velocity.

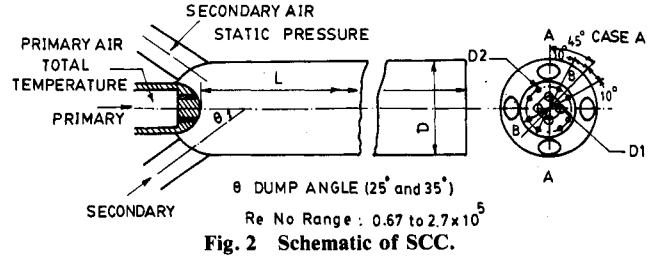


**Fig. 2 Schematic of SCC.**

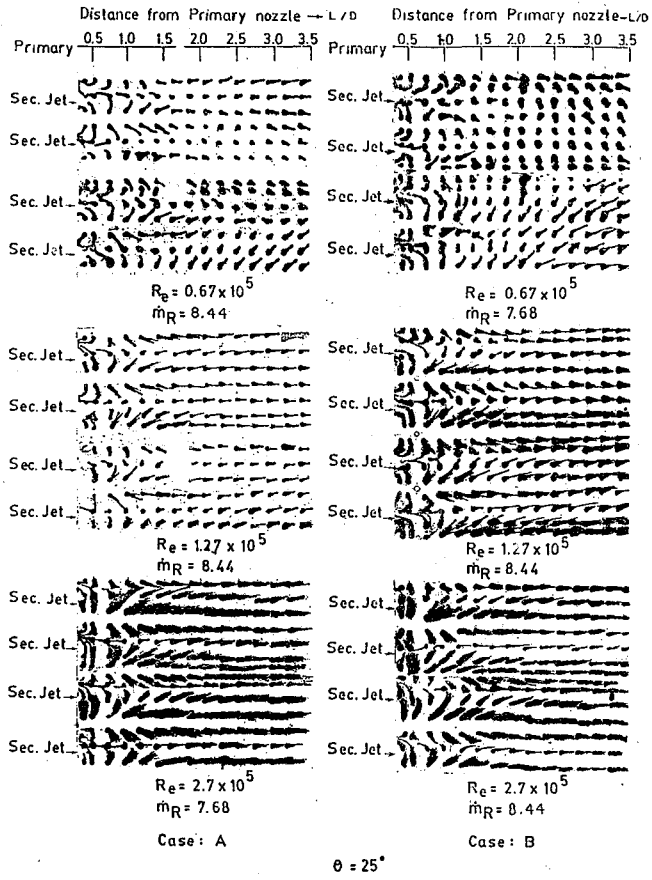


**Fig. 3 Surface flow patterns.**

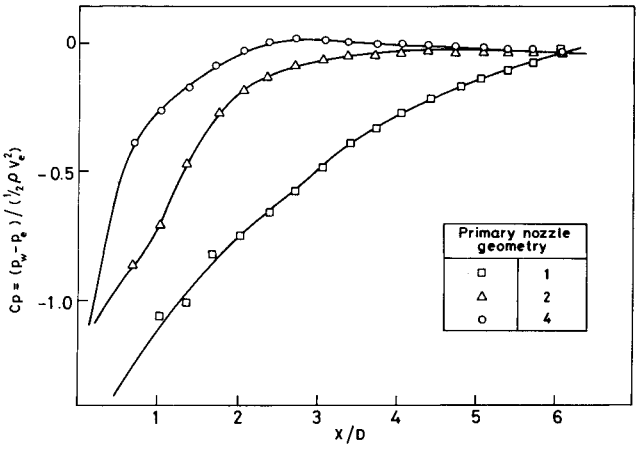


**Fig. 4 Wall static pressure along the combustion chamber length.**

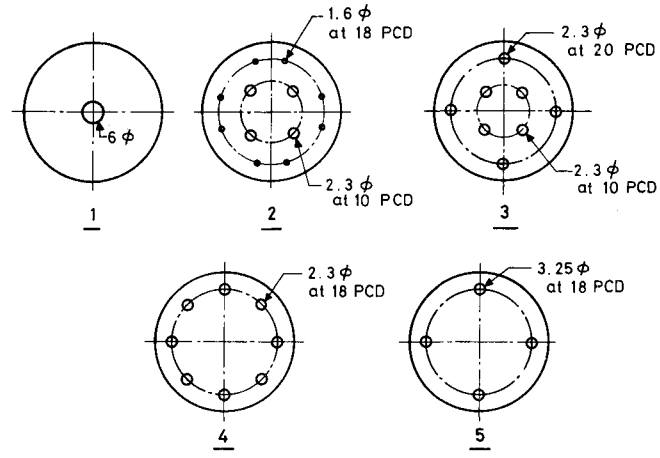


**Fig. 5 Various primary nozzle configurations.**

After the identity of the primary jet is lost, the pressure decreases due to frictional loss and increased velocity caused by the boundary-layer growth. The latter contribution has only a marginal influence for the length scales under consideration. Hence, the point of maximum wall static pressure gives an indication of the length required for the mixing of the primary and secondary jets. Ishikawa[8] plotted the wall pressure distribution along the combustor and concluded that the wall pressure maximum coincides with the reattachment point. This conclusion does not seem to be consistent with the present experimental results since from the surface flow visualization, the reattachment length was found to be about 1 diameter from the head end whereas the point of maximum static pressure varied from 2 to 6 diameters depending on the geometry.

### Temperature and Total Pressure

The mixing between the two jets can be assessed from the temperature and total pressure profiles at various axial locations. Figure 6 gives the radial temperature profiles at various axial locations, and Fig. 7 gives the corresponding total pressure profiles. The examination of the temperature profiles shows that the profiles become nearly flat at an $L/D$ of 5 for nozzle 2 (of Fig. 5) and at 3 for primary nozzle 4. Taking local temperature to be a direct indicator of local mixture ratio, the mixing efficiency at any section can be obtained by the relation

$$\eta_{\text{mix}} = 100\left[1 - \frac{\int_{A_L}(T_a - T)\,dA}{A_L(T_a - T_2)} - \frac{\int_{A_G}(T_a - T)\,dA}{A_G(T_a - T_1)}\right] \quad (1)$$

where $T_a$ is the average temperature (temperature the gas will attain when perfectly mixed), $T_1$ the temperature of the primary stream, and $T_2$ the temperature of the secondary stream. The $A_L$ is the area of that part of the cross section where $T$ is less than $T_a$ and $A_G$ the area where $T$ is greater than $T_a$. A more appropriate definition of mixing would have been obtained by taking mass flux weighted average rather than the simple area average as in Eq. (1). However, because the detailed mass flux distribution was not measured, simple area averaging was used. Nozzle 4 achieves 99% mixing at an $L/D$ of 3, and for nozzle 2 an $L/D$ of 5 is required for achieving the same mixing. These values match well with the point of maximum wall static pressure, which gives additional credence to the earlier proposition that the static pressure becomes maximum where mixing of the jets is nearly complete.

The total pressure profiles are plotted in Fig. 6. The points plotted are in the azimuthal position of maximum variation in total pressure. These profiles show considerable asymmetry and are not uniform even in the region where thermal mixing is complete. Hence in this situation the momentum and heat transfer seem to be considerably dissimilar.

### Momentum Loss

From mass conservation,

$$\dot{m}_p + \dot{m}_s = \dot{m}_c \quad (2)$$

From momentum conservation, the momentum loss due to friction is the difference between the momentum of the gases at the head end and that at the exit:

$$F_f = F_{\text{in}} - F_e \quad (3)$$

where

$$F_{\text{in}} = A_p P_p + \dot{m}_p V_p + (A_e - A_p)P_s + \dot{m}_s V_s \cos(\theta) \quad (4)$$

$$F_e = A_e P_e + \dot{m}_e V_e \quad (5)$$

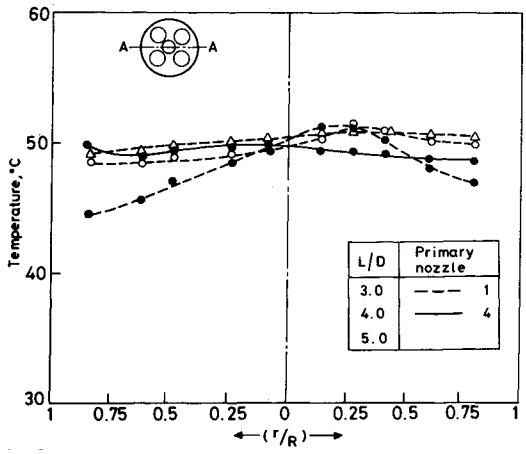


**Fig. 6 Temperature variation across the combustor at different axial locations.**

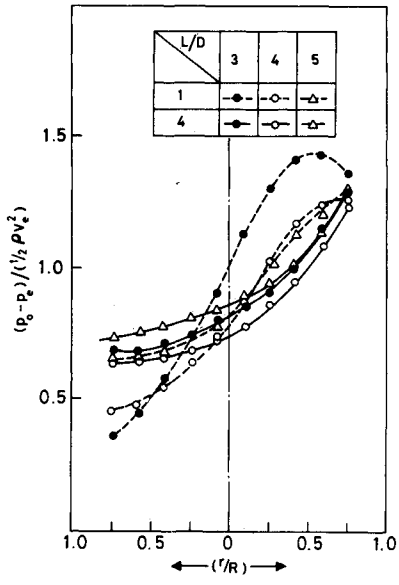


**Fig. 7 Total pressure variation across the combustor at different axial locations.**

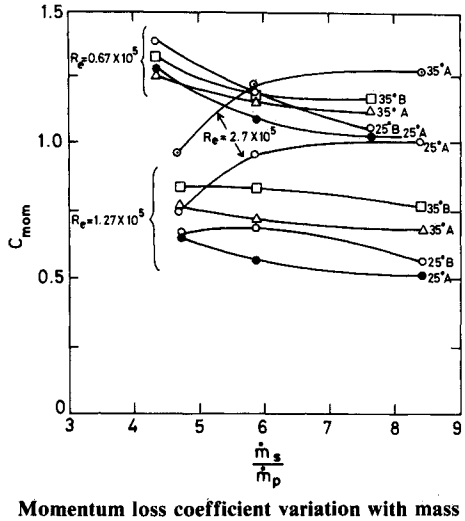


**Fig. 8 Momentum loss coefficient variation with mass flow ratio.**

where $\dot{m}_p$, $\dot{m}_s$, and $\dot{m}_c$ are the primary, secondary, and combustor total flow rate; and $F_f$, $F_{in}$, and $F_e$ are the momentum loss due to friction, momentum of the inlet jet and momentum of the exit jet, respectively.

The calculated values of the frictional force $F_f$ from the above equations is about 5–10 N for the range tested, which is between 3 to 5% of the inlet momentum. The corresponding total pressure loss due to friction will also be of the same order.

For the above calculation of the frictional momentum loss, the static pressure at the dome wall was assumed to be constant over the dome shape and equal to the secondary jet static pressure. However, there were some variations of the static pressure over the dome to the extent of 15%. When these variations were taken into account with the measured dome pressure values, the change in frictional loss was within 10% of the frictional loss calculated with uniform dome pressure. Since the total pressure loss due to friction is within 5%, the error introduced in calculating the combustion chamber total pressure using the above assumption is less than 0.5% (10% of 5%). Hence, the combustion chamber total pressure can be calculated fairly accurately assuming that the dome pressure equals the secondary jet pressure.

The momentum loss due to friction $F_f$ is nondimensionalized by the combustor exit dynamic head, and a momentum loss coefficient $C_{mom}$ has been defined as

$$C_{mom} = \frac{F_f}{(A\rho V^2/2)_e} \tag{6}$$

Figure 8 shows the variation of $C_{mom}$ with the mass flow ratio $\dot{m}_s/\dot{m}_p$ and dump angle for three Reynolds numbers for both cases A and B. Only case A has been shown for the highest Reynolds number.

In general, case A seems to have lower momentum loss. For the lower two Reynolds number cases, the momentum loss decreases with *Re* but increases for the highest Reynolds number. The result does not change with azimuthal angle.

**Table 1 Mixing length required for the various primary nozzles tested**

| Primary nozzle configuration number (Fig. 5) | Description | Hot/cold | *L/D* for mixing |
|---|---|---|---|
| 1 | Single hole of 6 mm | Cold | 7 |
| 2 | Eight holes of 1.6 mm at 18 mm *pcd* and four holes of 2.3 mm at 10 mm *pcd* | Cold<br>Hot | 5<br>5 |
| 3 | Four holes of 2.3 mm at 18 mm *pcd* and four holes of 2.3 mm at 10 mm *pcd* | Cold | 5 |
| 4 | Eight holes of 2.3 mm at 18 mm *pcd* | Cold<br>Hot | 2.8<br>2.8 |
| 4a | Same as above with 10-deg divergence | Cold | 2.8 |
| 5 | Four holes of 3.25 mm at 18 mm *pcd* | Cold | 3.6 |

### Effect of Primary Nozzle Configuration on Jet Mixing

The various primary nozzle configurations tested are shown in Fig. 5. Although it is to be expected that multiple primary jets give faster mixing, the distribution of holes, which gives the best performance, has not been reported in the earlier literature. The effect of primary nozzle configuration on jet mixing length is shown in Table 1. The *L/D* required for mixing varies from a high of 7 for single-hole nozzle to 2.8 for the multiple-hole nozzle of configuration 4 in Fig. 5. From the table, it is apparent that improved mixing is obtained by distributing the holes in the largest pitch circle diameter. Comparing the mixing length observed in configuration 6 with that observed in configurations 1 and 3 shows that the pitch circle diameter is more important than the number of holes. In the nozzle configurations 2 and 3, the holes are distributed on two pitch circles, and larger mixing lengths were observed in

both when compared to configuration 5, which had just four holes drilled on the large pitch circle of 2 and 3. For a constant pitch circle diameter, having a larger number of holes seems to provide better mixing as is evident from the comparison of configurations 4 and 5.

## Conclusions

1) The recirculation zone length is limited to an $L/D$ of 1–1.5 under most conditions of operation.

2) The total pressure loss due to friction was found to be within 5% of the total pressure for the range tested.

3) The choice of multiple-hole geometry reduces the combustion chamber length required for mixing of the jets. Having multiple holes at the largest pitch circle diameter seems to provide the best mixing configuration.

## Acknowledgment

The research work has been conducted under a project that has been supported by the Defense Research and Development Laboratory, Government of India, under the Joint Advanced Technology Program.

## References

[1]Buckley, R. R., and Obleskid, B. M., "The Effect of Swirl on a Ramjet Dump Combustor," AIAA Paper 79-7042, 1979.

[2]Yang, B. T., and Yu, M. H., "The Flow Field in a Suddenly Enlarged Combustion Chamber," *AIAA Journal,* Vol. 21, No. 1, 1983, pp. 92–97.

[3]Da-ming, C., Yue-Ying, O., and Zhen-Zong, S., "Preliminary Experimental Study of Combustion in the Solid Rocket-Ramjet," Fifth International Society of Air Breathing Engines Meeting, AIAA, New York, 1981.

[4]Zitterstrom, K. A., Sjoblom, B., and Jarnmo, A., "Solid Ducted Rocket Engine Combustion Tests," AIAA Paper 83-7001, 1983.

[5]Hsia, H. T., and Dunlap, R., "A Parametric Study of Secondary Combustion," *Acta Astronautica,* 1971, pp. 127–136.

[6]Masuya, G., Chinzie, N., and Ishii, S., "A Study of Air Breathing Rockets—Subsonic Mode Combustion," *Acta Astronautica,* Vol. 8, No. 4, 1981, pp. 643–661.

[7]Greenberg, J. B., and Timnat, Y. M., "Sudden Expansion Injection for Ram-Rockets," Fifth International Society of Air Breathing Engines Meeting, AIAA, New York, 1981.

[8]Ishikawa, N., "Experimental Study of Jet Mixing Mechanisms in a Model Secondary Combustor," *AIAA Journal,* Vol. 21, 1983, pp. 565–571.

[9]Tsujikado, N., "An Experimental Study on Configuration of Secondary Combustion Chamber for Ram-Rocket," Sixth International Society of Air Breathing Engine Meeting, AIAA, New York, 1983.

[10]Ramanujachari, V., Krishnan, S., Padiyar, K. S., Natarajan, R., and Gupta, M. C., "Performance Analysis of Primary and Secondary Systems of Rocket Ramjet Engine Burning Fuel-Rich Metallised Propellants," Fifth International Society of Air Breathing Engines Meeting, AIAA, New York, 1981.

[11]Cohen, N. S., "Combustion Considerations in Fuel-Rich Propellant Systems," *AIAA Journal,* Vol. 7, No. 7, 1969, pp. 1345–1352.